

## LETTER TO THE EDITOR

# Effect of Substitution of $\text{Cr}^{3+}$ in Place of $\text{Mn}^{3+}$ in Rare-Earth Manganates on the Magnetism and Magnetoresistance: Role of Superexchange Interaction and Lattice Distortion in $\text{LnMn}_{1-x}\text{Cr}_x\text{O}_3$ <sup>1</sup>

R. Gundakaram, Anthony Arulraj, P. V. Vanitha, and C. N. R. Rao<sup>2</sup>

*Solid State and Structural Chemistry Unit, Indian Institute of Science, Bangalore 560 012, India*

N. Gayathri and A. K. Raychaudhuri

*Department of Physics, Indian Institute of Science, Bangalore 560 012, India*

and

A. K. Cheetham

*Materials Research Laboratory, University of California, Santa Barbara, California 93106*

Communicated by J. M. Honig October 29, 1996; accepted November 7, 1996

Magnetic and electrical properties of oxides of the formula  $\text{LnMn}_{1-x}\text{Cr}_x\text{O}_3$  ( $\text{Ln}$  = rare earth) have been investigated to understand the importance of the  $\text{Mn}^{3+}\text{--O--Cr}^{3+}$  superexchange interactions, in contrast to the  $\text{Ln}_{1-x}\text{A}_x\text{MnO}_3$  ( $\text{A}$  = divalent cation) system, where double exchange interactions predominate. All the  $\text{LnMn}_{1-x}\text{Cr}_x\text{O}_3$  compositions are ferromagnetic insulators and exhibit small values of negative magnetoresistance (MR) at ordinary temperatures, the highest value of MR at 6 T being  $\sim 20\%$  at 120 K for some of the compositions. The results underscore the important role of double exchange, as well as lattice distortion effects, in giving rise to high values of MR in  $\text{Ln}_{1-x}\text{A}_x\text{MnO}_3$ . © 1996 Academic Press

Rare-earth manganates of the type  $\text{Ln}_{1-x}\text{A}_x\text{MnO}_3$  ( $\text{Ln}$  = rare earth;  $\text{A}$  = divalent cation) become ferromagnetic near a critical value of  $x$  and exhibit an insulator–metal transition close to the Curie temperature (1). These properties are explained based on the double exchange mechanism for electron hopping between  $\text{Mn}^{3+}$  and  $\text{Mn}^{4+}$  ions (2). These manganates also exhibit giant magnetoresistance (GMR), the magnitude being highest close to  $T_c$  (3–6). The GMR in these materials has also been explained on the basis of double exchange, along with other factors

(7, 8). In particular, lattice distortions arising from the local Jahn–Teller (JT) distortion of the  $\text{Mn}^{3+}$  ion play a key role in electron transport as well as in magnetic exchange. The origin of the large MR in the  $\text{La}_{1-x}\text{A}_x\text{MnO}_3$  observed near  $T_c$  is partly due to the forced alignment of the local  $t_{2g}$  core spins by the application of a magnetic field, causing a reduction in the spin disorder scattering of the  $e_g$  electrons. It is also possible that near  $T_c$ , the onset of ferromagnetic order and application of a magnetic field give rise to spin-ordering, which, in turn, leads to a reduction in the local distortion, thereby causing delocalization of carriers and reduction of resistivity. It is to be noted that the  $\text{Mn}^{3+}\text{--O--Mn}^{4+}$  superexchange interaction is ferromagnetic, unlike the antiferromagnetic  $\text{Mn}^{3+}\text{--O--Mn}^{3+}$  and  $\text{Mn}^{4+}\text{--O--Mn}^{4+}$  superexchange interactions. We considered it most interesting to examine the magnetic and electrical properties of rare-earth manganates where  $\text{Mn}^{3+}$  is partly substituted by  $\text{Cr}^{3+}$  as in  $\text{LnMn}_{1-x}\text{Cr}_x\text{O}_3$ , since  $\text{Cr}^{3+}$  has the same  $t_{2g}^3$  electronic configuration as  $\text{Mn}^{4+}$  but has a larger ionic radius. The  $\text{Mn}^{3+}\text{--O--Cr}^{3+}$  superexchange interaction would be ferromagnetic (9), but there would be no double exchange interaction, as in the case of the  $\text{Ln}_{1-x}\text{A}_x\text{MnO}_3$  system containing  $\text{Mn}^{3+}\text{--O--Mn}^{4+}$  units. The  $\text{Cr}^{3+}$  ion with a larger radius than  $\text{Mn}^{4+}$  would lower the tolerance factor  $t$ , leading to a greater distortion from the ideal cubic structure.

We have prepared several  $\text{LnMn}_{1-x}\text{Cr}_x\text{O}_3$  ( $\text{Ln}$  = La, Pr, Nd, and Gd) derivatives ensuring the absence of  $\text{Mn}^{4+}$

<sup>1</sup> Supported by the Jawaharlal Nehru Centre for Advanced Scientific Research.

<sup>2</sup> To whom correspondence should be addressed.

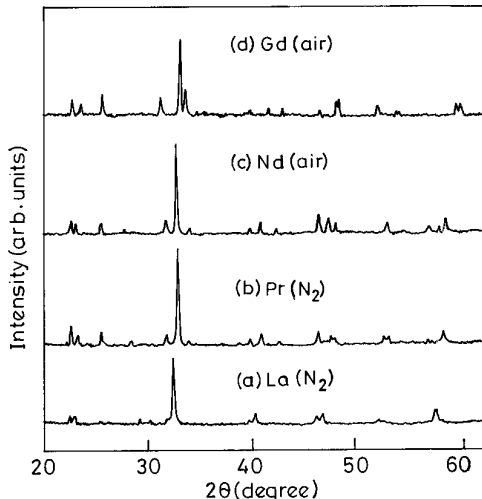


FIG. 1. X-ray diffractograms of the  $LnMn_{0.7}Cr_{0.3}O_3$  compositions.

(in order to eliminate the possibility of double exchange interaction) and investigated their magnetic and electrical properties, including the magnetoresistance behavior, in order to delineate the importance of double exchange and superexchange interactions in determining the GMR and related properties of the manganates. While the present study does indeed show the  $LnMn_{1-x}Cr_xO_3$  derivatives to be ferromagnetic, with  $T_c$  depending on  $x$  and  $Ln$ , they are all highly insulating and do not show the characteristic insulator–metal transition at  $T_c$  seen in the double exchange manganates. These materials also do not show appreciable magnetoresistance, thus underscoring the important role of double exchange in giving rise to GMR in  $La_{1-x}A_xMnO_3$ .

All  $LnMn_{1-x}Cr_xO_3$  derivatives were prepared by the solid

state reaction of the rare-earth oxides with  $MnCO_3$  and  $Cr_2O_3$ .  $LaMn_{1-x}Cr_xO_3$  compositions prepared in this manner by heating in air at 1370 K for 32 h showed significant amounts of  $Mn^{4+}$  as determined by redox titrations. The  $Mn^{4+}$  content decreases with an increase in  $x$ . Thus, the  $Mn^{4+}$  content was 5% when  $x = 0.2$  and close to 0% when  $x = 0.3$ . In order to be absolutely certain that no  $Mn^{4+}$  was present, we prepared the  $LaMn_{1-x}Cr_xO_3$  ( $x = 0.1$  to  $0.3$ ) compositions by heating in nitrogen at 1370 K for 32 h. Although this method may result in a slight oxygen deficiency, it ensures that both Mn and Cr are in their maximum formal oxidation state of  $3^+$ . The same procedure was followed to prepare  $PrMn_{0.7}Cr_{0.3}O_3$ , the  $x = 0.3$  composition being preferred since  $Mn^{4+}$  is not favored at this Cr content.  $NdMn_{0.7}Cr_{0.3}O_3$  and  $GdMn_{0.7}Cr_{0.3}O_3$  prepared in air showed no trace of  $Mn^{4+}$ ; the heavier rare earths generally do not seem to favor the formation of  $Mn^{4+}$ .

All the  $LnMn_{1-x}Cr_xO_3$  compositions had the orthorhombic structure, with the exception of  $LaMn_{0.8}Cr_{0.2}O_3$  prepared in air. We show typical X-ray diffraction patterns of the  $LnMn_{0.7}Cr_{0.3}O_3$  compositions in Fig. 1 and list the unit cell parameters in Table 1 along with the  $Mn^{4+}$  content. In the table, we also indicate the kind of orthorhombic structure adopted by these solids. The O-type orthorhombic perovskite structure ( $a < c\sqrt{2} < b$ ) supports ferromagnetic exchange, but may not exhibit a clear Jahn–Teller distortion. The O'-type structure ( $c/\sqrt{2} < a < b$ ) leads to ordering of the  $e_g$  electrons of  $Mn^{3+}$  on the B sites and to an anisotropic magnetic exchange. As the  $Mn^{4+}$  content increases in  $Ln_{1-x}A_xMnO_3$  the structural distortion decreases and one obtains a rhombohedral structure when  $\% Mn^{4+} \geq 20$  ( $t \geq 0.9$ ). Strong ferromagnetism (highest  $T_c$ ) and the onset of metallic state (below  $T_c$ ) are seen in the rhombohedral structure. Although  $Cr^{3+}$  has the same

TABLE 1  
Properties of  $LnMn_{1-x}Cr_xO_3$  Compositions

$Ln$	$x$ ( $t$ )	% $Mn^{4+}$	Lattice parameters			$\Theta$ (K) <sup>c</sup>	$T_c$ (K) <sup>d</sup>	$E_a$ (eV)
			$a$	$b$	$c$ (Å) <sup>b</sup>			
La (air)	0.2	5	5.472 <sup>a</sup>	—	—	206	216	0.123
	0.3 (0.897)	0	5.489	5.519	7.775 (O)	209	221	0.116
La (N <sub>2</sub> )	0.1 (0.892)	0	5.524	5.643	7.733 (O')	108	152	0.122
	0.2 (0.894)	0	5.518	5.634	7.755 (O')	118	137	0.118
	0.3 (0.897)	0	5.522	5.614	7.765 (O')	118	128	0.115
Pr (N <sub>2</sub> )	0.3 (0.896)	0	5.446	5.646	7.641 (O')	100	89	0.257
Nd (air)	0.3 (0.890)	0	5.417	5.619	7.763 (O)	63	73	0.186
Gd (air)	0.3 (0.871)	0	5.319	5.709	7.529 (O)	−10	32	—

<sup>a</sup> Rhombohedral,  $\alpha = 60.6^\circ$ .

<sup>b</sup> O and O' shown in parentheses indicate the type of the orthorhombic structure.

<sup>c</sup> Paramagnetic Curie temperatures obtained by extrapolation of  $1/\chi$  vs  $T$  curves.

<sup>d</sup> Estimated from  $\chi$ - $T$  curves.

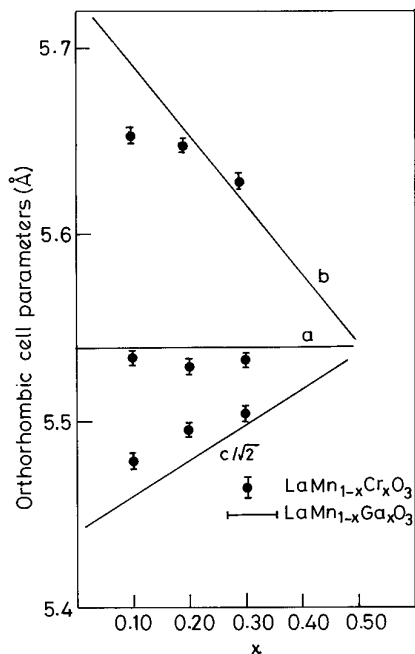


FIG. 2. Variation in the orthorhombic cell parameters of  $\text{LaMn}_{1-x}\text{Cr}_x\text{O}_3$  with  $x$ . The full line corresponds to the data on  $\text{LaMn}_{1-x}\text{Ga}_x\text{O}_3$  (10). Note that diamagnetic  $\text{Ga}^{3+}$  has the same radius as  $\text{Cr}^{3+}$ .

electronic structure as  $\text{Mn}^{4+}$ , it does not reduce the lattice distortion sufficiently to effect a transition to the rhombohedral structure, thereby inhibiting the onset of the metallic state below  $T_c$ . The larger ionic radius of  $\text{Cr}^{3+}$  (relative to  $\text{Mn}^{4+}$ ) and lower  $t$  may be responsible for the retention of the orthorhombic structure. We see from Table 1 that even with 30%  $\text{Cr}^{3+}$ ,  $t < 0.9$ . The orthorhombic lattice parameters of  $\text{LaMn}_{1-x}\text{Cr}_x\text{O}_3$  vary with  $x$ , just as those of  $\text{LaMn}_{1-x}\text{Ga}_x\text{O}_3$  (10), as shown in Fig. 2, suggesting the  $B$ -ion radius to be the crucial factor.

In Fig. 3, we show the dc magnetic susceptibility data of the  $\text{LaMn}_{1-x}\text{Cr}_x\text{O}_3$  compositions prepared in air as well as in nitrogen. The susceptibilities of the  $\text{LnMn}_{0.7}\text{Cr}_{0.3}\text{O}_3$  ( $\text{Ln} = \text{La}, \text{Pr}, \text{Nd}, \text{and Gd}$ ) compositions were similar, characteristic of ferromagnetic materials. The paramagnetic Curie temperatures,  $\Theta$ , obtained by the extrapolation of the inverse susceptibility data are generally positive (Table 1). We also list the approximate ferromagnetic  $T_c$  values in this table. For the  $\text{LaMn}_{1-x}\text{Cr}_x\text{O}_3$  compositions,  $T_c$  decreases with an increase in  $x$ , due to the increasing  $\text{Cr}^{3+}\text{-O-Cr}^{3+}$  antiferromagnetic (AFM) interaction. In  $\text{LnMn}_{0.7}\text{Cr}_{0.3}\text{O}_3$ ,  $T_c$  decreases as we go down the rare-earth series ( $\text{La} > \text{Pr} > \text{Nd} > \text{Gd}$ ). The  $A$ -type AFM structure of  $\text{LaMnO}_3$  is destroyed by the  $\text{Cr}^{3+}$  substitution (this is similar to the  $\text{Mn}^{4+}$  substitution in  $\text{La}_{1-x}\text{A}_x\text{MnO}_3$ ), and the  $G$ -type AFM spin structure of  $\text{LaCrO}_3$  appears when  $x \approx 0.4$  (11). In the  $x = 0.1\text{--}0.3$  range investigated by us, antiferromagnetic layers with ferromagnetically aligned moments coexist with a ferrimagnetic phase. The suscepti-

bility behavior of  $\text{LaMn}_{0.7}\text{Cr}_{0.3}\text{O}_3$  suggests ferrimagnetic behavior at low temperatures. The existence of mixed exchange as well as competing types of AFM order in Cr-rich and Mn-rich regions render the magnetic characterization complex. What stands out, however, is that below a certain temperature (designated as  $T_c$ ) there is an alignment of ferromagnetic moments. Introduction of  $\text{Cr}^{3+}$  into the  $A$ -type AFM structure of  $\text{LaMnO}_3$  can cause spin-realignment of one or more of its  $\text{Mn}^{3+}$  neighbors, leading to a ferromagnetic moment. This has implications on the magnetoresistance, as pointed out later.

In Fig. 4, we present the temperature variation of the electrical resistivity ( $\rho$ ) of  $\text{LaMn}_{1-x}\text{Cr}_x\text{O}_3$  and  $\text{LnMn}_{0.7}\text{Cr}_{0.3}\text{O}_3$ . All these materials are good insulators and do not show metal-insulator transitions at  $T_c$ , unlike  $\text{La}_{1-x}\text{A}_x\text{MnO}_3$ . The room temperature resistivities are typically in the range of 1–15 ohm cm. The resistivities of the  $\text{LaMn}_{1-x}\text{Cr}_x\text{O}_3$  compositions (prepared in nitrogen) decrease with increasing  $x$ .  $\text{GdMn}_{0.7}\text{Cr}_{0.3}\text{O}_3$  showed much too large a resistivity at room temperature; no attempt was therefore made to measure its temperature dependence of resistivity. The resistivity of  $\text{LnMn}_{1-x}\text{Cr}_x\text{O}_3$  varies as  $\text{Gd} > \text{Nd} > \text{Pr} > \text{La}$ . The insulating behavior of the ferromagnetic  $\text{LnMn}_{1-x}\text{Cr}_x\text{O}_3$  derivatives illustrates that without double exchange there can be no metallicity in the orthorhombic manganates. Ferromagnetism in the Cr-substituted compositions, arising only from the superexchange interaction, does not produce a metallic state. The resistivity of all the samples follows simple activated behavior; the activation energies,  $E_a$ , show a systematic trend (Table 1). As the lattice distortion decreases in  $\text{LaMn}_{1-x}\text{Cr}_x\text{O}_3$  with increasing  $x$ ,  $E_a$  decreases perceptibly.  $\text{NdMn}_{0.7}\text{Cr}_{0.3}\text{O}_3$  and  $\text{PrMn}_{0.7}\text{Cr}_{0.3}\text{O}_3$ , which have smaller  $t$  values, exhibit larger  $E_a$  values. The values of  $E_a$  for

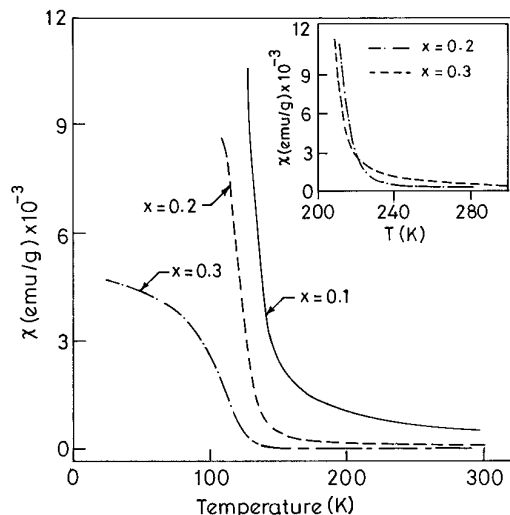


FIG. 3. Temperature variation of the dc magnetic susceptibility of  $\text{LaMn}_{1-x}\text{Cr}_x\text{O}_3$  compositions prepared in nitrogen. Inset shows the data for the  $x = 0.2$  and  $0.3$  compositions prepared in air.

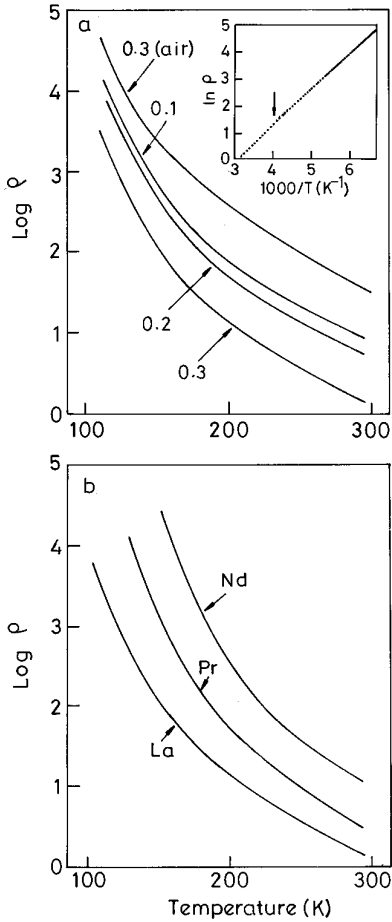


FIG. 4. Electrical resistivity data (a) for  $\text{LaMn}_{1-x}\text{Cr}_x\text{O}_3$  and (b)  $\text{LnMn}_{0.7}\text{Cr}_{0.3}\text{O}_3$ . The inset in (a) shows the plot of  $\log(\rho)$  vs  $1/T$  for  $\text{LaMn}_{0.7}\text{Cr}_{0.3}\text{O}_3$ . Note the change in slope around 240 K.

$\text{LaMn}_{1-x}\text{Cr}_x\text{O}_3$  are comparable to those of  $\text{La}_{1-x}\text{A}_x\text{MnO}_3$  (at  $T > T_c$ ).

The absence of double exchange interaction in  $\text{LnMn}_{1-x}\text{Cr}_x\text{O}_3$  shows up clearly in the magnetoresistance data. We have measured the magnetoresistance (MR) of the various  $\text{LnMn}_{1-x}\text{Cr}_x\text{O}_3$  derivatives by the four-probe method in magnetic fields up to 6 T generated using a superconducting solenoid (5). We show the temperature variation of MR in Fig. 5. All the compounds show negative MR. However, the magnitude is small. It should, however, be kept in mind that the MR has been measured only down to 100 K. Generally, in the manganates containing  $\text{Mn}^{4+}$ , the value of MR peaks close to  $T_c$ . For most of the samples measured by us, except  $\text{PrMn}_{0.7}\text{Cr}_{0.3}\text{O}_3$  and  $\text{NdMn}_{0.7}\text{Cr}_{0.3}\text{O}_3$ ,  $T_c \geq 100$  K. It is therefore reasonable to conclude that MR is unlikely to attain much larger values at lower temperatures. In fact, the  $\text{LaMn}_{1-x}\text{Cr}_x\text{O}_3$  samples show a tendency for saturation around 100 K. In  $\text{PrMn}_{0.7}\text{Cr}_{0.3}\text{O}_3$  and  $\text{NdMn}_{0.7}\text{Cr}_{0.3}\text{O}_3$  with  $T_c < 100$  K, MR is low, the magnitude being lower in the latter composition with a lower  $T_c$ .

The temperature dependence of MR of  $\text{LaMn}_{1-x}\text{Cr}_x\text{O}_3$  (Fig. 5) is not monotonic. The value of MR increases in two distinct steps, one occurring around 250 K, and the other occurring around  $T_c$  (marked by arrows in Fig. 5). The increase in MR close to  $T_c$  is expected but the small distinct step around 250 K deserves attention. We have indeed observed a decrease ( $\sim 12\%$ ) in the activation energy as  $\text{LaMn}_{0.7}\text{Cr}_{0.3}\text{O}_3$  is cooled through 250 K, as shown in the inset of Fig. 4. This behavior probably arises from the local ferromagnetically aligned clusters of spins. Substitution of  $\text{Cr}^{3+}$  in place of  $\text{Mn}^{3+}$  gives rise to a FM interaction through  $\text{Mn}^{3+}-\text{O}-\text{Cr}^{3+}$  superexchange, and to a strong AFM interaction through  $\text{Cr}^{3+}-\text{O}-\text{Cr}^{3+}$  superexchange. When  $x \leq 0.3$ , this may lead to local spin-aligned clusters arising from a  $\text{Cr}^{3+}$  ion surrounded by six  $\text{Mn}^{3+}$  ions. For higher values of  $x$ , two or more  $\text{Cr}^{3+}$  ions can be immediate neighbors, favoring AFM over the ferromagnetic alignment of spins. The formation of local clusters of ferromagnetically aligned spins can lead to a decrease in  $E_a$  and to an enhancement of negative MR near a temperature

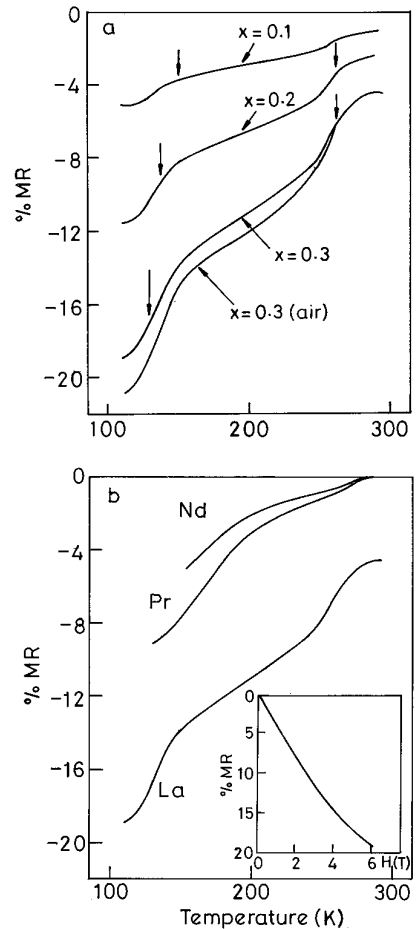


FIG. 5. Temperature variation of magnetoresistance (MR) of (a)  $\text{LaMn}_{1-x}\text{Cr}_x\text{O}_3$  and (b)  $\text{LnMn}_{0.7}\text{Cr}_{0.3}\text{O}_3$  in a field of 6 T. Inset in (b) shows the variation of MR with the magnetic field in  $\text{LaMn}_{0.7}\text{Cr}_{0.3}\text{O}_3$ .

corresponding to the cluster formation. We suggest that this occurs around 250 K in  $\text{LaMn}_{0.7}\text{Cr}_{0.3}\text{O}_3$ , leading to the observed changes in  $E_a$  and MR.

The absence of proper spin-ordering due to the coexistence of a strong AFM interaction is also seen in the magnetic-field dependence of the MR at a fixed temperature (see inset in Fig. 5b). The field-dependence of MR in ferromagnetic  $\text{La}_{1-x}\text{A}_x\text{MnO}_3$  with proper spin alignment generally shows two-step behavior (5): a sharp rise in MR at low fields, typically  $H < 1$  T, followed by a slow change at higher fields. The gradual variation of MR with H, showing no approach to saturation in fields as high as 6 T, indicates that the present material lacks proper spin alignment.

In conclusion, we find that ferromagnetic superexchange interactions arising from  $\text{Mn}^{3+}-\text{O}^{2-}-\text{Cr}^{3+}$  units do not lead to strong ferromagnetic ordering, metallic behavior, and giant magnetoresistance in  $\text{LnMn}_{1-x}\text{Cr}_x\text{O}_3$ . This is to be contrasted with the isoelectronic  $\text{Mn}^{3+}-\text{O}-\text{Mn}^{4+}$  units in  $\text{La}_{1-x}\text{A}_x\text{MnO}_3$  which give rise to novel transport properties due to the strong ferromagnetic double exchange interactions, as well as the larger tolerance factor (due to the smaller ionic size of  $\text{Mn}^{4+}$ ), which reduces the lattice distortion and enhances the bandwidth.

## ACKNOWLEDGMENTS

The authors thank the Indo-French Center for Advanced Research and the MRL Program of the National Science Foundation under Award DMR9123048 for support of this research.

## REFERENCES

1. G. H. Jonker and J. H. Van Santen, *Physica* **16**, 337 (1950); J. H. Van Santen and G. H. Jonker, *Physica* **16**, 599 (1950).
2. C. Zener, *Phys. Rev.* **82**, 403 (1951).
3. K. Chahara, T. Ohno, M. Kasai, and Y. Kozono, *Appl. Phys. Lett.* **63**, 1990 (1993).
4. R. von Helmolt, B. Holzapfel, L. Schultz, and K. Samwer, *Phys. Rev. Lett.* **71**, 2331 (1993).
5. R. Mahesh, R. Mahendiran, A. K. Raychaudhuri, and C. N. R. Rao *J. Solid State Chem.* **114**, 297 (1995); R. Mahendiran, S. K. Tiwary, A. K. Raychaudhuri, T. V. Ramakrishnan, R. Mahesh, N. Rangavittal, and C. N. R. Rao, *Phys. Rev. B* **53**, 3348 (1996).
6. C. N. R. Rao and A. K. Cheetham, *Science* **272**, 369 (1996) and the references cited therein.
7. N. Furukawa, *J. Phys. Soc. Jpn.* **63**, 3214 (1994).
8. A. J. Millis, P. B. Littlewood, and B. I. Shraiman, *Phys. Rev. Lett.* **74**, 5144 (1995); *Phys. Rev. B* **53**, 8434 (1996).
9. G. H. Jonker, *Physica* **22**, 707 (1956).
10. J. B. Goodenough, A. Wold, R. J. Arnott, and N. Menyuk, *Phys. Rev.* **124**, 373 (1961).
11. U. H. Bent, *Phys. Rev.* **106**, 225 (1957).